

SYNTHESIS OF GRAPHENE OXIDE-TiO₂ NANOTUBES-SILVER NANOPARTICLES NANOCOMPOSITE BY GAMMA IRRADIATION FOR ANTIBACTERIAL AND POST-HARVEST PRESERVATION PURPOSES

Nguyen Thi Phuong Anh¹, Pham Thi Thuy Loan², Nguyen Vu Duy Khang¹, Vo Nguyen Dang Khoa^{1,2} ✉

¹Institute of Applied Materials Science, Vietnam Academy of Science and Technology

²Graduate University of Science and Technology, Vietnam Academy of Science and Technology

✉To whom correspondence should be addressed. E-mail: vndkhoa@iams.vast.vn

Received: 19.11.2019

Accepted: 23.12.2019

SUMMARY

In this study, graphene oxide (GO)-TiO₂ nanotubes (TNTs)-silver nanoparticles (AgNPs) nanocomposites were synthesized under γ -ray irradiation at different doses (5, 10, 15, 20 and 25 kGy) from formerly synthesized GO, TNTs and AgNPs. They were then characterized by Fourier-transformed infrared (FTIR) and ultra-violet-visible (UV-Vis) spectroscopies, as well as by scanning electron (SEM) and transmission electron (TEM) microscopes. The spectral data indicated the assemblage of silver nanoparticles on both GO sheets and TiO₂ nanotubes, as well as the assemblage of TiO₂ nanotubes on GO sheets. In addition, their antibacterial activity against *Escherichia coli* and post-harvest preservation were investigated. Fresh bunches of green grapes were used for this study. AATCC 100-2012 and ISO 21527-1:2008 standards were used for all experiments. The obtained results indicated that all nanocomposite samples exhibited very high antibacterial activity against *E. coli*. Among which, the 20 kGy sample showed the highest value. Moreover, two samples (5 kGy and 25 kGy) possessed the lower number of yeasts and molds than that of control sample, indicating that the nanocomposites had partial contribution to the preservation of post-harvest crops. We have also found in this study that the dose range affected the antibacterial activity and preservation; and the highest dose range, however, was not always ideal for that purpose. With such fascinating properties, GO-TNTs-AgNPs will be the promising material for antibacterial and agricultural applications.

Keywords: Graphene oxide, TiO₂ nanotubes, silver nanoparticles, *Escherichia coli*, nanocomposite, post-harvest crops

INTRODUCTION

Graphene oxide (GO), with the sheet structure assembled with oxygen-bearing functional groups, has been known for more than fifty years (Hummers *et al.*, 1958). It has, however, never been obsolete for scientific studies, thanks to the outstanding mechanical strength, electrical and thermal conductivities, molecules barrier properties and other remarkable abilities (Cui *et al.*, 2016; Smith *et al.*, 2019). The release of ROS (reactive oxygen species) of GO is the descent of its capability of interacting with many types of chemical and biological molecules such as DNA or RNA. Bykkam *et al.* (2013) demonstrated that GO, in nanoparticles form, exhibited very good antibacterial activity against *Klebsiella pneumoniae* and *Staphylococcus aureus*. In

addition, Gupta *et al.* (2015) reported that GO binds with lipopolysaccharides in the cell surface of bacteria through exogenous oxygenated functional groups to form hydroxyl bonds. These results indicated the potential of GO as an antibacterial material.

Titanium dioxide (TiO₂), especially TiO₂ nanotubes (TNTs), has been widely known as among the best photo-catalysts for contamination treatments and solar energy harvesting. Moreover, this material, comparing with nanoparticles, possess higher specific surface area, with orderly one-dimensional structure, hence their spectacular photocatalytic activity. According to Kunrath *et al.* (2019), TNTs are friendly to organisms and they show relatively good antibacterial activity, which can be enhanced by

combining with other metal particles. The mechanism antibacterial activity of TNTs' was explained by Li *et al.* (2019) as two routes: the endurance and subsequent spillage of bacteria's membrane into the TiO₂ nanotubes, and the subsidence of water from bacteria's membrane, resulting in their contraction and death.

Beside fascinating physical and chemical properties, silver nanoparticles (AgNPs), especially in the size range of 10 to 100 nm (Selim *et al.*, 2018), exhibit strong antibacterial activity, hence their wide application being an effective bactericide. They are capable of reacting with sulfur-containing amino acids, inside or outside the cell membrane, and affecting the cell viability. In addition, silver ions (Ag⁺) released from AgNPs can interact with phosphorous moieties in DNA molecules, leading to the inactivation of DNA replication and malfunction of proteins.

With all fascinating properties of GO, TNTs and AgNPs themselves, in this study, we have synthesized the GO-TNTs-AgNPs nanocomposite and evaluated its antibacterial activity for the potential of usage in crops post-harvest preservation.

MATERIALS AND METHODS

Graphite powder was purchased from ACROS ORGANICS (Germany), silver nitrate (AgNO₃), nitric acid 65 % and TiO₂ anatase nanopowder were purchased from MERCK (Germany). All other chemicals were in analytical pure grade and deionized water was used throughout the work. GO were synthesized using the method published by Marcano *et al.* (2010), using graphite powder as precursor and potassium permanganate as oxidizer. Silver nanoparticles (AgNPs) were synthesized using the method published by Aherne *et al.* (2008), with polyethylene glycol (PEG) as the substitute for poly(sodium styrenesulfonate) (PSSS). TiO₂ nanotubes (TNTs) were synthesized based on the method published by Zavala *et al.* (2017), using TiO₂ anatase nanopowder as titania precursor.

After that, GO and TNTs were dispersed separately in a PEG 0.5 g.L⁻¹ solution by sonication for 30 minutes and then mixed with each other. The mixture was then joined by AgNPs solution followed by another 30 minutes of sonication. The GO-AgNPs-TNTs mixtures were then γ -irradiated by the COBALT-60/B irradiator, at the dose range of 5, 10, 15, 20 and 25 kGy. The products were labeled 5, 10,

15, 20 and 25 kGy, respectively.

All nanocomposite samples were characterized by Fourier-transformed infrared (FTIR) and ultra violet-visible (UV-Vis) spectroscopies, on a PerkinElmer MIR/NIR Frontier spectrometer for FTIR and UV-1800 (Shimadzu, Japan) spectrometer for UV-Vis. For the SEM and TEM imaging, a FE SEM S-4800 microscope (Hitachi, Japan) and a JEOL JEM-1400 (JEOL, USA) were used.

For antibacterial activity investigation, all experiments were conducted at the Laboratory of Animals Biotechnology – Faculty of Biology and Biotechnology – University of Science – VNU-HCM, following the AATCC 100-2012: Antibacterial Finishes on Textile Material standard. The procedure was repeated three times for all samples. The antibacterial percent (R) was then determined for all samples following the formula as following:

$$R = [(B-A)/B] \times 100\%$$

Whereas A is the total number of *E. coli* colonies in nanocomposite samples from three times of repetition and B is that of the control sample

For the investigation the role of nanocomposites on post-harvest preservation, 2 mg of all nanocomposites were completely dispersed in appropriate amount of deionized water and sprayed on the crop surface. Bunches of fresh green grapes (White Malaga variety, originated from Thailand) were picked up from different places in the field, in Ninh Thuan Province, Vietnam. After discarding bruised ones, grapes were washed, dried and preserved under ambient condition and one week later they were tested for presence of yeast (*Saccharomyces cerevisiae*) and mold (*Botrytis cinerea*), following the ISO 21527-1:2008 standard. The experiments were conducted at the TSL Testing Center, Ho Chi Minh City.

RESULTS AND DISCUSSION

Nanocomposites characterization

After being irradiated by γ -ray with different doses, all nanocomposite solutions were obtained as dark brown solution (Figure 1).

In the FTIR spectra (Figure 2), it could be observed as a broad peak at ~3400 cm⁻¹ for the hydroxyl (O-H) group; a strong peak at ~1700 cm⁻¹ for the carbonyl (C=O) groups and Ti-O bonds (Manalu *et al.*, 2018), as well as weak signals of C-

O single bonds (carboxy, alkoxy and epoxy) and C≡C bonds from 1000 to 1400 cm^{-1} . These signals were typical for GO and TNTs, comparing to those of bare materials. Noticeably, the signals at $\sim 3400 \text{ cm}^{-1}$ and $\sim 1700 \text{ cm}^{-1}$ were also present in bare AgNPs sample. These signals resembled those obtained in the study of Sharma *et al.* (2014) and they were revealed to belong to the organic media of AgNPs solution. In our case, it can be inferred that the signal at $\sim 3400 \text{ cm}^{-1}$ belonged to the hydroxyl groups of both water and PEG molecules, while the other one at $\sim 1700 \text{ cm}^{-1}$ belonged to the carbonyl groups formed by the change of PEG molecules after exposing to γ -irradiation.

Moreover, in all irradiated samples, a broad peak in the range of 800-400 cm^{-1} was also present, resembling that of bare AgNPs. According to Alsharaeh *et al.* (2017), there were similarities in the obtained nanocomposites' spectra, indicating that this broad peak was the signal of Ti-O-Ti stretching and Ag-O bond. The lattice vibration signal of TiO_2 at $\sim 1400 \text{ cm}^{-1}$ became absent in the nanocomposite samples, hence the possible interaction between Ag and TiO_2 (Alsharaeh *et al.* (2017)). The higher the irradiation dose was, the stronger effect they exhibited towards interaction between GO, AgNPs and TNTs, hence the stronger signals obtained.

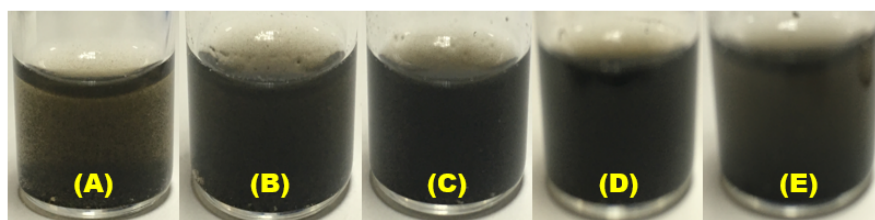


Figure 1. Irradiated nanocomposite solution at the dose of 5 kGy (A); 10 kGy (B); 15 kGy (C); 20 kGy (D); and 25 kGy (E)

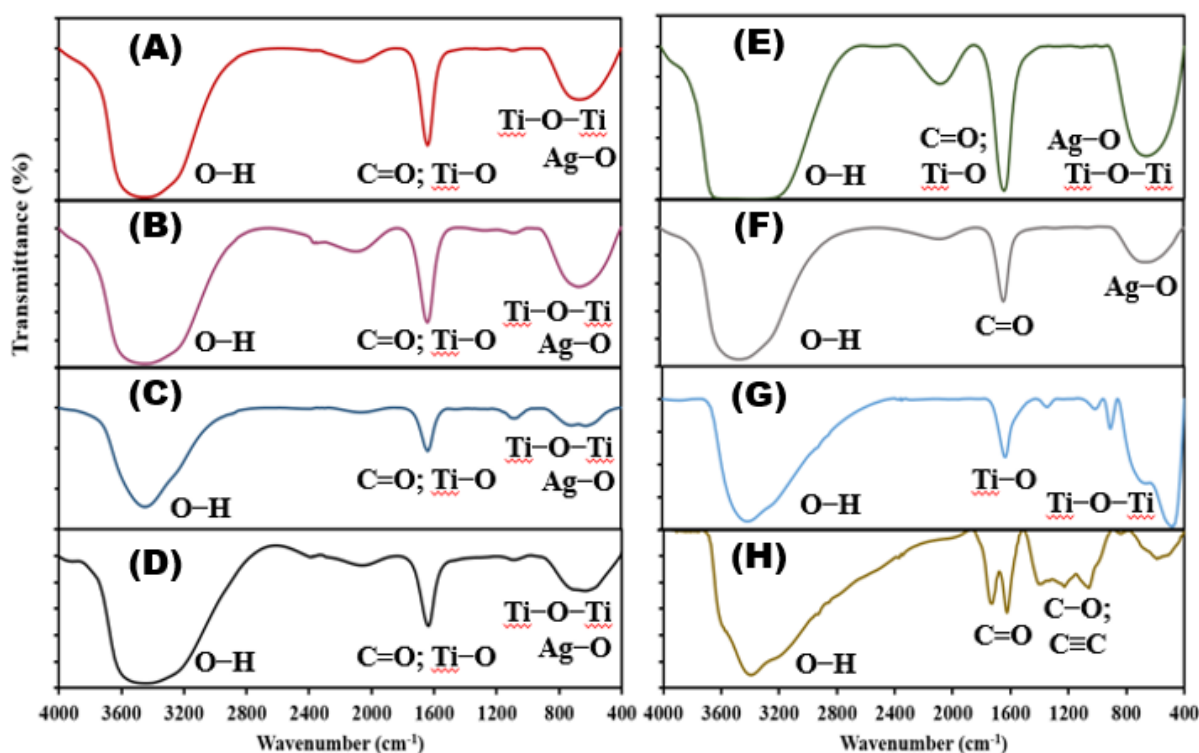


Figure 2. FTIR spectra of nanocomposite samples at the dose of 5 kGy (A); 10 kGy (B); 15 kGy (C); 20 kGy (D); and 25 kGy (E), compared with that of AgNPs (F); TNTs (G); and GO (H).

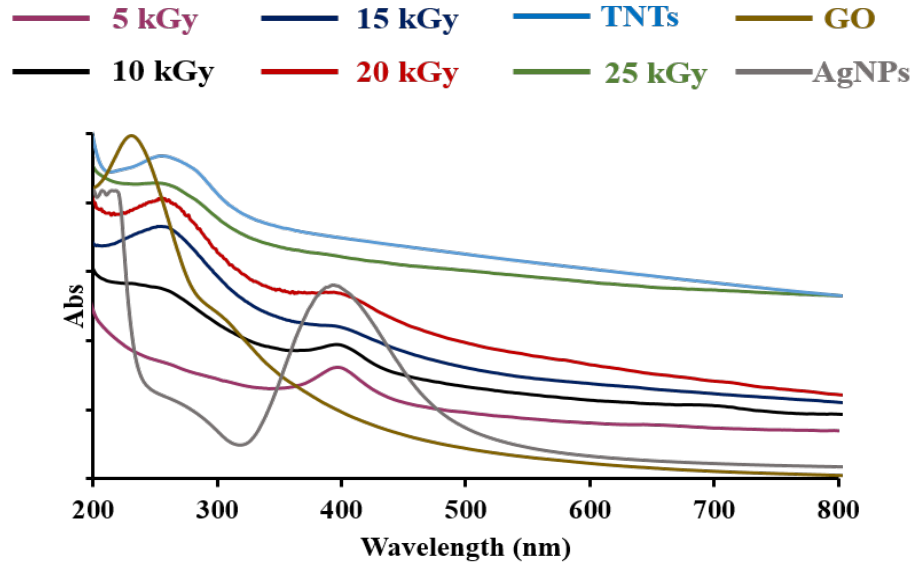


Figure 3. UV-Vis adsorption spectra of nanocomposite samples at the dose of 5 kGy; 10 kGy; 15 kGy; 20 kGy; and 25 kGy, compared with that of AgNPs; TNTs; and GO.

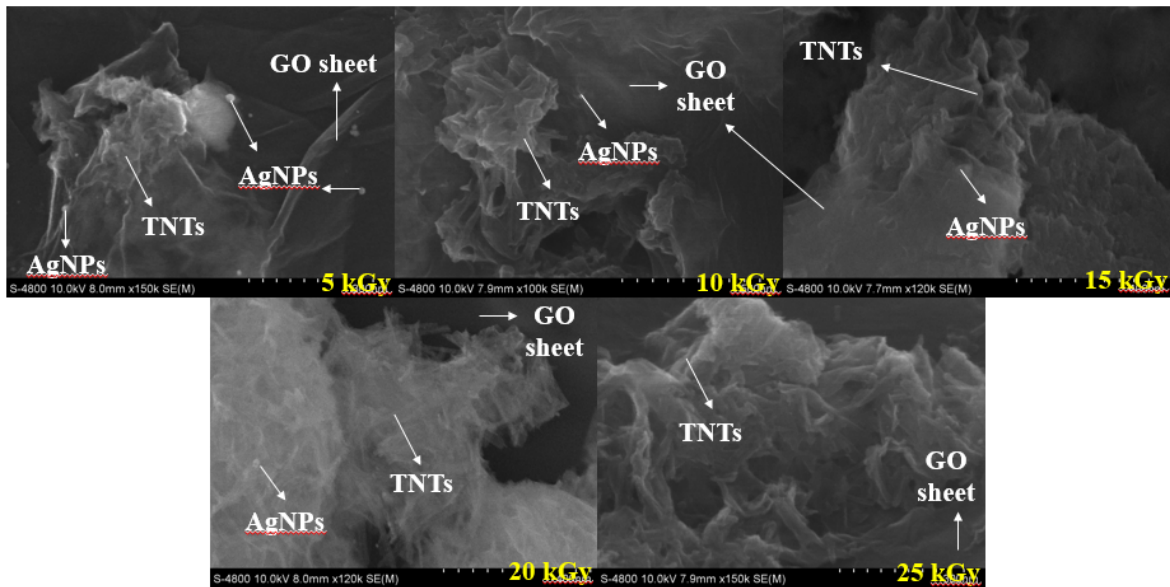


Figure 4. SEM images of nanocomposite samples at the dose of 5 kGy; 10 kGy; 15 kGy; 20 kGy; and 25 kGy, with indicated GO, AgNPs, and TNTs components.

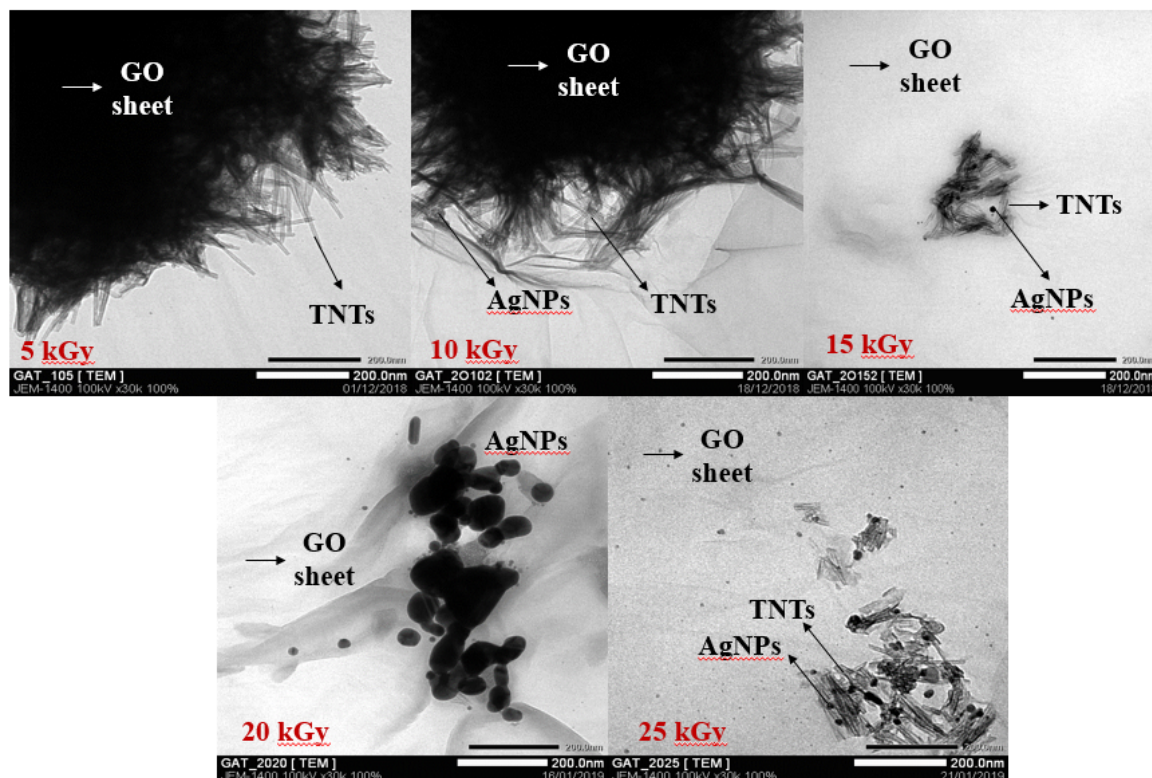


Figure 5. TEM images of nanocomposite samples at the dose of 5 kGy; 10 kGy; 15 kGy; 20 kGy; and 25 kGy, with indicated GO, AgNPs, and TNTs components.

The UV-Vis adsorption spectra (Figure 3) indicated that the UV-Vis adsorption properties of nanocomposites and bare materials were different, which reinforced our prediction that under γ -ray irradiation, there were bindings formed between GO, AgNPs and TNTs. In details, the adsorption peak of GO (at ~ 240 nm) disappeared in the nanocomposites, of which possible cause is the attachment of AgNPs and TNTs on GO's surface (Chen *et. al.*, 2016). Secondly, it was obvious that the higher the dose was, the weaker the AgNPs adsorption peak (at ~ 400 nm) was. This result could be explained that at high doses of γ -irradiation, PEG molecules were degraded and lost the protective effect on silver nanoparticles, caused them to aggregate and form larger particles, with different UV-Vis adsorption properties. Similar trend was observed in the study of Chen *et. al.* (2007). The signal of TNTs at ~ 270 nm became stronger as the irradiation dose augmented, due to the higher crystallization of TiO₂ nanotubes under γ -ray exposure. Together with obtained FTIR spectra, these results indicated that GO, AgNPs and TNTs actually

interacted with each other to form the nanocomposite products under γ -ray irradiation.

Figure 4 and 5 displayed the SEM and TEM images of GO-AgNPs-TNTs nanocomposite materials. Except the highest dose (25 kGy), GO, TNTs and AgNPs could be observed in the SEM images, with the TNTs distributed on the GO sheets and loaded by AgNPs. Some of AgNPs were assembled directly on the GO's surface. The absence of AgNPs in the image of the 25 kGy sample was due to the agglomeration of AgNPs under high irradiation dose, making them more difficult to be observed. These SEM images demonstrated the successful synthesis of GO-TNTs-AgNPs nanocomposites. Similar trend was observed clearly on TEM images, with TNTs distributed and covered by layers of GO sheets, as well as AgNPs assemblage on the GO's surface and TiO₂ nanotubes. The image of 20 kGy sample also showed the agglomeration of AgNPs under high irradiation dose, with larger particles than other samples.

Antibacterial activity investigation

Figure 6 is the images of *E. coli* colonies after culturing with the presence of nanocomposites, together with the control sample. It was obvious that there were very few *E. coli* colonies present in all nanocomposites, comparing with the control sample, indicating the very high antibacterial activity.

The R value of nanocomposites were shown in Table 1.

Results in Table 1 indicated that all nanocomposite samples exhibited antibacterial activity against *E. coli*, among which the highest value belongs to the 20 kGy sample. Moreover, it can be inferred from these values that the highest irradiation dose does not mean the highest antibacterial activity. From the irradiation dose of 5 kGy to 15 kGy, the higher the dose was, the lower

the R value was, which was contradictory to the dose of 20 kGy. The tendency was similar from the dose of 20 kGy and 25 kGy. This variation can be explained as following: from 5 kGy to 15 kGy, the higher the dose was, the stronger the TiO₂ nanotubes crystallization and silver nanoparticles agglomeration was; this, therefore, diminish the number of reactive locations on both TNTs and GO, hence the decrease in antibacterial activity. At the dose of 20 kGy, which is high enough for breaking some bonds between GO, AgNPs and TNTs, some silver nanoparticles released, leaving new reactive locations on the surface of TNTs and GO and increasing the antibacterial activity. As the dose augmented from 20 to 25 kGy, the promotion of remaining TNTs crystallization and AgNPs agglomeration continued, resulted in the diminution of antibacterial activity.

Table 1. Antibacterial percent (R) values of nanocomposites.

Sample	<i>E. coli</i> colonies	A	B	R (%)
5 kGy	0	5	-	99.33 ± 0.20
	3		-	
	2		-	
10 kGy	3	11	-	98.53 ± 0.15
	5		-	
	3		-	
15 kGy	7	22	-	97.07 ± 0.08
	8		-	
	7		-	
20 kGy	0	1	-	99.87 ± 0.08
	1		-	
	0		-	
25 kGy	1	3	-	99.60 ± 0.02
	1		-	
	1		-	
Control	250	-	750	-
	250	-		
	250	-		

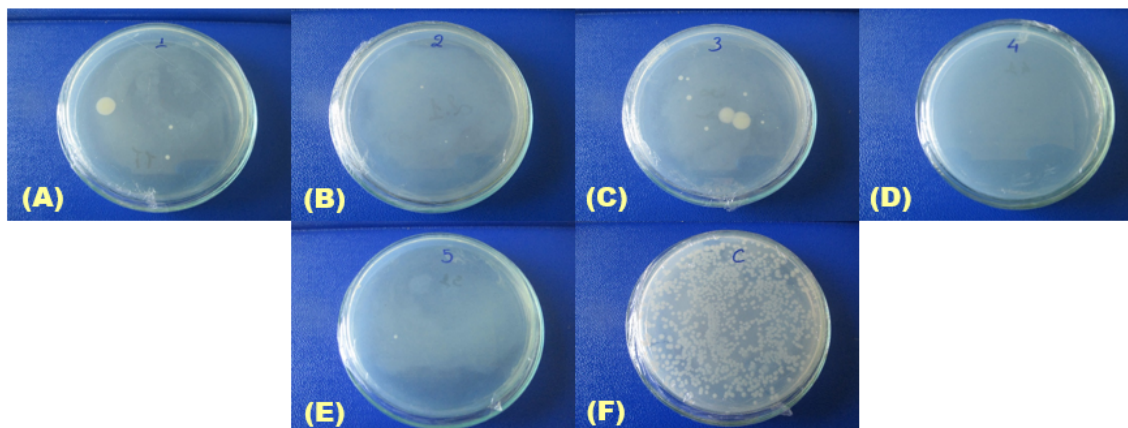


Figure 6. Images of *E. coli* colonies in nanocomposite samples at the dose of 5 kGy (A); 10 kGy (B); 15 kGy (C); 20 kGy (D); 25 kGy (E); and control sample (F).

Crops post-harvest preservation investigation

The enumeration of yeasts and molds of all samples after being treated with nanocomposite samples and one week of preservation under ambient conditions were shown in Table 2.

Results in Table 2 showed that only two nanocomposites-treated grape bunches possessed lower yeast and mold spores number than that of the control sample, and the sample whose

antibacterial activity was the highest (the 20 kGy sample) was not the one with the lowest number of yeast and mold spores. Our explanation for these results was that the GO-AgNPs-TNTs nanocomposites exhibited different activity against fungi species from *E. coli*, of which cause is the difference in the binding manner between GO, AgNPs and TNTs. In addition, the augmentation in irradiation dose does not lead to the increase in inhibiting ability of nanocomposites.

Table 2. Enumeration of yeasts and molds in grape bunches (control and nanocomposites-treated samples).

Sample	Number of yeast and mold spores (CFU.g ⁻¹)
5 kGy	$(1.4 \pm 0.38) \times 10^3$
10 kGy	$(8.7 \pm 0.11) \times 10^4$
15 kGy	$(3.4 \pm 0.13) \times 10^4$
20 kGy	$(2.0 \pm 0.10) \times 10^4$
25 kGy	$(2.2 \pm 0.29) \times 10^3$
Control	6.0×10^3

CONCLUSION

In this study, the nanocomposite materials composed of GO, TNTs and AgNPs was synthesized by γ -irradiation at different doses. The spectral characterization of these nanocomposites indicated the attachment of silver nanoparticles on both surface of GO sheets and TiO₂ nanotubes, and of TiO₂ surface of GO sheets. The antibacterial activity of GO-TNTs-

AgNPs against *E. coli* was spectacular, and this material possessed a particular contribution to the preservation of crops under ambient conditions. For further study, we will focus on the antibacterial activity of GO-AgNPs-TNTs against other species of bacteria and fungi, and determine of remaining nanocomposites on the crops after washing with water before consumption.

Acknowledgement: *This research is funded by Vietnam National Foundation for Science and Technology Development (NAFOSTED) under grant number 104.03-2017.49 and by Vietnam Academy of Science and Technology (VAST) under grant number VAST.ĐLT.06/16-17*

REFERENCES

Aherne D, Ledwith DM, Gara M, Kelly JM (2008) Optical properties and growth aspects of silver nanoparticles produced by a highly reproducible and rapid synthesis at room temperature. *Adv Funct Mater* 18: 2005-2016

Alsharaeh EH, Bora T, Soliman A, Ahmed F, Bhrarath G, Ghoniem MG, Abu-Salah KM, Dutta J (2017) Sol-gel-assisted microwave-derived synthesis of anatase Ag/TiO₂/GO nanohybrids toward efficient visible light phenol degradation. *Catalysts* 7: 1-10

Bykkam S, Rao VK, Chakra CHS, and Thumgunta T (2013) Synthesis and characterization of graphene oxide and its antimicrobial activity agents *Klebsiella* and *Staphylococcus*. *Int J Adv Biotech & Res* 1(4): 142-146

Chen D, Zou L, Li S, Zheng F (2016) Nanospherical like reduced graphene oxide decorated TiO₂ nanoparticles: an advanced catalyst for the hydrogen evolution reaction. *Sci Rep* 6(20335): 1-9

Chen P, Song L, Liu Y, Fang Y (2007) Synthesis of silver nanoparticles by γ -ray irradiation in acetic water solution containing chitosan. *Radiat Phys Chem* 76: 1165-1168.

Cui Y, Kundalwal S, Kumar S (2016) Gas barrier performance of graphene/polymer nanocomposites. *Carbon* 98: 313-333

Gupta DK, Rajaura RS, Jasuja ND, Sharma K (2015) Synthesis and characterization of graphene oxide nanoparticles and their antibacterial activity. *Environ Sci Technol* 1(1): 16-24

Hummers WS, Offeman RE (1958) Preparation of graphitic oxide. *J Am Chem Soc* 1339-1339

Kunrath MF, Leal BF, Hubler R, de Oliveira SD, Teixeira ER (2019) Antibacterial potential associated with drug-delivery built TiO₂ nanotubes in biomedical implants. *AMB Expr* 9(51): 1-13

Li Y, Yang Y, Li R, Tang X, Guo D, Qing Y, Qin Y (2019) Enhanced antibacterial properties of orthopedic implants by titanium nanotube surface modification: a review of current techniques. *Int J Nanomed* 14: 7217-7236

Manalu SP, Natarajan TS, De Guzman M, Wang YF, Chang TC, Yen FC, You SJ (2018) Synthesis of ternary g-C₃N₄/Bi₂MoO₆/TiO₂ nanotube composite photocatalysts for the decolorization of dyes under visible light and direct sunlight irradiation. *Green Process Synth* 7(6): 493-505

Marcano DC, Kosynkin DV, Berlin JM, Sinitskii A, Sun Z, Slesarev A, Alemany LB, Lu W, Tour JM (2010) Improved Synthesis of Graphene Oxide. *ACS Nano* 4(8): 4806-4814

Selim A, Elhaig MM, Taha SA, Nasr EA (2018) Antibacterial activity of silver nanoparticles against field and reference strains of *Mycobacterium tuberculosis*, *Mycobacterium bovis* and multiple-drug-resistant tuberculosis strains. *OIE Rev Sci Tech* 37(3): 1-16

Sharma G, Sharma AR, Kurian M, Bhavesh R, Nam JS, Lee SS (2014) Green synthesis of silver nanoparticles using *Myristica fragrans* (Nutmeg) seed extract and its biological activity. *Dig J Nanomater Bios* 9(1): 325-332

Smith AT, LaChance AM, Zeng S, Liu B, Sun L (2019) Synthesis, properties, and applications of graphene oxide/reduced graphene oxide and their nanocomposites. *Nano Mater Sci* 1(1): 31-47

Zavala MAL, Ávila-Santos M (2017) Synthesis of stable TiO₂ nanotubes: effect of hydrothermal treatment, acid washing and annealing temperature. *Heliyon* 3(2017): 1-18

TỔNG HỢP VẬT LIỆU TỔ HỢP GRAPHENE OXIDE-ỐNG NANO TiO₂-NANO BẠC BẰNG PHƯƠNG PHÁP CHIẾU XẠ GAMMA DÙNG TRONG KHÁNG KHUẨN VÀ BẢO QUẢN NÔNG SẢN SAU THU HOẠCH

Nguyễn Thị Phương Anh¹, Phạm Thị Thúy Loan², Nguyễn Vũ Duy Khang¹, Võ Nguyễn Đăng Khoa^{1,2}

¹*Viện Khoa học Vật liệu Ứng dụng, Viện Hàn lâm Khoa học & Công nghệ Việt Nam*

²*Học viện Khoa học và Công nghệ, Viện Hàn lâm Khoa học & Công nghệ Việt Nam*

TÓM TẮT

Trong nghiên cứu này, vật liệu tổ hợp graphene oxide (GO), ống nano TiO₂ (TNTs) và nano bạc (AgNPs) được tổng hợp bằng phương pháp chiếu xạ tia γ với những liều xạ khác nhau (5, 10, 15, 20 và 25 kGy) từ các vật liệu thành phần tương ứng. Các mẫu vật liệu tổ hợp được khảo sát tính chất bằng các phương pháp phổ hồng ngoại (FTIR), phổ hấp thụ tử ngoại-khả kiến (UV-Vis), ảnh chụp kính hiển vi điện tử quét (SEM) và kính hiển

vi điện tử truyền qua (TEM). Kết quả thu được cho thấy các hạt nano bạc bám trên cả các tấm GO và ống nano TiO₂, đồng thời các ống TiO₂ gắn trên bề mặt các tấm GO. Bên cạnh đó, hoạt tính kháng khuẩn *Escherichia coli* và bảo quản nông sản sau thu hoạch của vật liệu tổ hợp cũng đã được khảo sát. Nho xanh được sử dụng làm đối tượng khảo sát trong nghiên cứu này. Các thí nghiệm đánh giá hoạt tính tuân theo tiêu chuẩn AATCC 100-2012 và ISO 21527-1:2008. Kết quả cho thấy tất cả các mẫu vật liệu tổ hợp đều thể hiện hoạt tính kháng khuẩn *E. coli* cao, trong đó mẫu 20 kGy là cao nhất. Ngoài ra, chỉ có hai mẫu (5 và 25 kGy) có tổng số nấm men, nấm mốc thấp hơn mẫu đối chứng. Điều này vừa cho thấy vật liệu tổ hợp GO-TNTs-AgNPs có tác động nhất định đến quá trình bảo quản nông sản sau thu hoạch, vừa cho thấy liều chiếu xạ cao nhất không phải là lý tưởng nhất. Với những tính chất thú vị này, vật liệu hứa hẹn sẽ có nhiều áp dụng cho mục đích kháng khuẩn và sử dụng trong nông nghiệp.

Từ khóa: *Graphene oxide, ống nano TiO₂, nano bạc, Escherichia coli, vật liệu tổ hợp, nông sản sau thu hoạch*